



**HAL**  
open science

## Modified 3D-printed device for mercury determination in waters

Elodie Mattio, Nadia Ollivier, Fabien Robert-Peillard, Robert Di Rocco,  
André Margaillan, Christophe Brach-Papa, Joel Knoery, Damien Bonne,  
Jean-Luc Boudenne, Bruno Coulomb

### ► To cite this version:

Elodie Mattio, Nadia Ollivier, Fabien Robert-Peillard, Robert Di Rocco, André Margaillan, et al..  
Modified 3D-printed device for mercury determination in waters. *Analytica Chimica Acta*, Elsevier  
Masson, 2019, 1082, pp.78-85. 10.1016/j.aca.2019.06.062 . hal-02284950

**HAL Id: hal-02284950**

**<https://hal-amu.archives-ouvertes.fr/hal-02284950>**

Submitted on 12 Sep 2019

**HAL** is a multi-disciplinary open access archive for the deposit and dissemination of scientific research documents, whether they are published or not. The documents may come from teaching and research institutions in France or abroad, or from public or private research centers.

L'archive ouverte pluridisciplinaire **HAL**, est destinée au dépôt et à la diffusion de documents scientifiques de niveau recherche, publiés ou non, émanant des établissements d'enseignement et de recherche français ou étrangers, des laboratoires publics ou privés.

Copyright

## Modified 3D-printed device for mercury determination in waters

Elodie Mattio<sup>1</sup>, Nadia Ollivier<sup>1</sup>, Fabien Robert-Peillard<sup>1</sup>, Robert Di Rocco<sup>1</sup>, Catherine Branger<sup>2</sup>, André Margaillan<sup>2</sup>, Christophe Brach-Papa<sup>3</sup>, Joël Knoery<sup>3</sup>, Damien Bonne<sup>4</sup>, Jean-Luc Boudenne<sup>1</sup>, Bruno Coulomb<sup>1\*</sup>

<sup>1</sup> Aix Marseille Univ, CNRS, LCE, Marseille, France.

<sup>2</sup> University of Toulon, MAPIEM, La Garde, France.

<sup>3</sup> IFREMER, LBCM, Nantes, France.

<sup>4</sup> Aix Marseille Univ, CNRS, Centrale Marseille, ISM2, Marseille, France.

\*Corresponding author: bruno.coulomb@univ-amu.fr

Full postal address: LCE, Case 29, 3 place Victor Hugo, 13331 Marseille cedex 3, France.

### Abstract

3D printing technology is increasingly used in flow analysis, to develop low cost and tailor-made devices. The possibility of grafting specific molecules onto 3D printed parts offers new perspectives for the development of flow systems. In this study, a MPFS system including a dicarboxylate 1,5-diphenyl-3-thiocarbazone grafted 3D-printed device has been developed for mercury determination. For this purpose, the surface of 3D-printed cuboids was first modified with amine functional groups and then grafted with dicarboxylate 1,5-diphenyl-3-thiocarbazone. This new grafted device resulted in selective mercury preconcentration with extraction and elution yields higher than 90% even at high sampling flow rates. The detection can then be carried out in two ways: a direct detection of mercury extracted onto 3D-printed grafted cuboids by atomic absorption spectrophotometry after amalgam on gold or a detection of mercury in solution after elution with L-cysteine by spectrophotometry or cold vapor atomic absorption spectrometry.

Keywords: stereolithography; Poly(MethylMethacrylate) grafting; dicarboxylate 1,5-diphenyl-3-thiocarbazone; Multi Pumping Flow System; mercury.

### Introduction

Mercury is one of the most toxic metal, present in the environment in different chemical forms. This post-transition metal has a high toxicity at low levels and may accumulate in organisms [1] which increases its dangerousness. The exposition to mercury can cause damages to organs [2] as respiratory and kidney diseases, dysfunctions of the nervous system [3,4] with memory troubles and developmental delay for exposed children, or troubles in the development of foetus. Mercury has the capacity to be exchanged between the different reservoirs of the biosphere [5], whether in organic or in inorganic form. There are few natural sources of mercury such as volcanism and geothermal sources [6], while anthropogenic sources are very important: mining, combustion of fossil fuels [7,8], production of batteries from mercury oxide, use in electrolytic processes for chemical or pesticides production. A recent study [9] estimated anthropic mercury in the environment at 1 540 000 tonnes, of which 73% was emitted between 1850 and 2010.

44 In the light of its toxicity and its numerous sources of pollution, the World Health Organization  
45 has recommended a guideline value of  $6 \mu\text{g L}^{-1}$  for inorganic mercury in drinking water and  
46 European regulations have set a maximal allowable concentration (MAC) in natural waters at  
47  $0.07 \mu\text{g L}^{-1}$  for mercury and its compounds. Accordingly, the development of simple, rapid and  
48 sensitive methods for on-line Hg determination in natural waters has attracted widespread  
49 attention in modern analytical chemistry. Flow analysis seems to be appropriate to meet these  
50 specific requirements: this technology allows the decrease of instrumentation size and of  
51 reagents and energy consumption, which are significant advantages to simplify the  
52 manipulations required for the assays.

53 Many flow systems have been developed for quantification of mercury in waters, with a  
54 detection step often performed by cold vapor atomic absorption spectrometry (CV-AAS) [10-  
55 12]. Colorimetric detection has been also used for high concentrations of mercury [13,14].  
56 Independently of the detection method, the quantification of low levels of mercury is usually  
57 difficult because of sample storage problems [15]. A portable analytical system would avoid  
58 these problems, but the coupling with complex laboratory detection techniques (atomic  
59 absorption spectrometry (AAS), inductively coupled plasma mass spectrometry (ICP-MS) or  
60 inductively coupled plasma atomic emission spectrometry (ICP-AES)) would remain difficult  
61 to handle. A colorimetric detection step may be considered if a pre-concentration module is  
62 used for low mercury concentrations.

63 3D printing eases the creation of three-dimensional custom fluidic modules as columns and  
64 mixers and several flow systems based on such 3D-printed modules have been reported  
65 previously for the determination of lead [16], cadmium [17] or chromium [18].

66 In this study, the 3D printing resin was used directly after the photopolymerization process as  
67 a support for the grafting of a ligand for the selective extraction of mercury. Dicarboxylate 1,5-  
68 diphenyl-3-thiocarbazone (DTZc) was chosen for this purpose because of its affinity for  
69 mercury [19]. The grafting procedure is performed in two stages: first, amine functions are  
70 integrated on the surface of the photopolymerized resin and then dicarboxylate 1,5-diphenyl-3-  
71 thiocarbazone is grafted by reaction between its carboxylic function and the amine function  
72 added to the resin. Various detection methods have been considered and several applications  
73 are discussed here as examples to illustrate the opportunity of using a 3D printed grafted  
74 module.

75

## 76 **2. Materials and methods**

### 77 **2.1. Reagents and solutions**

78 All chemicals used were of analytical grade and used without further purification. Solutions  
79 were prepared with ultra-pure water (Millipore, resistivity  $> 18 \text{ M}\Omega \text{ cm}$ ) and stocked in high  
80 density polyethylene or Teflon flasks. Mercury standard solutions were prepared by dilution of  
81 a commercial  $1 \text{ g.L}^{-1}$  AAS mercury stock solution (Fisher Chemical, USA) and stabilized with  
82 1% v/v nitric acid trace metal grade (Fisher Chemical, USA).

83 A multi-metal solution ( $10 \mu\text{mol.L}^{-1}$  for each metal) was prepared by diluting and mixing eleven  
84 commercial AAS stock solutions of aluminium, cadmium, calcium, cobalt, copper, iron, lead,  
85 magnesium, mercury, silver and zinc at  $1 \text{ g.L}^{-1}$  (Fisher Chemical, USA) in ultra-pure water.

86 Modification of 3D printed devices was carried out with hexane diamine (Fisher Chemical,  
87 USA), N-(3-Dimethylaminopropyl)-N'-ethylcarbodiimide (EDC, GenScript, USA) and 1-  
88 Hydroxybenzotriazole (HOBt, Fluka, USA).

89 Detection was performed by two techniques: spectrophotometric detection with a reagent  
90 composed of dithizone (Sigma-Aldrich, USA) and thiourea (Sigma-Aldrich, USA) prepared in  
91 a glycine buffer solution (Sigma-Aldrich, USA) in 30% absolute ethanol v/v (Sigma-Aldrich,  
92 USA), whereas hydrochloric trace metal grade (Fisher Chemical, USA) and sodium  
93 borohydride (Sigma-Aldrich, USA) were prepared in hydroxide solution (Fisher Chemical,  
94 USA) for CV-AAS detection.

95

## 96 2.2 Synthesis of DTZc

97 Dicarboxylate 1,5-diphenyl-3-thiocarbazon (DTZc) was synthesized following the conditions  
98 defined by Shenashen et al. [19]. Briefly, 1.9 g of hydrazinobenzoic acid were mixed with 0.6  
99 mL of carbon disulfide, 20 mL of ethanol, 0.5 g of sodium hydroxide and 15 mL of distilled  
100 water. The mixture was heated to reflux for 5 hours; then DTZc was precipitated as a white  
101 solid by addition of ethanol, filtered, washed and dried. The reaction yield was 22% (0.95 g of  
102 dicarboxylate 1,5-diphenyl-3-thiocarbazon).

103

## 104 2.3 Modification of 3D printed device

105 3D printed devices were post-processed by cleaning in isopropyl alcohol for 10 minutes and  
106 curing for 1 hour under UV light. Integration of amine functions was carried out by immersion  
107 of 3D printed post-cured parts for 1 h in a 10% m/v solution of hexane diamine prepared in a  
108 solution of borate buffer adjusted to pH 11.5. The aminated parts were carefully cleaned by  
109 successive baths in water, in ethanol and in water afresh. The DTZc grafting was then carried  
110 out by immersion in a mixture of 5 g.L<sup>-1</sup> solution of N-(3-Dimethylaminopropyl)-N'-  
111 ethylcarbodiimide (EDC), 5 g.L<sup>-1</sup> solution of 1-Hydroxybenzotriazole (HOBt) and 1 g.L<sup>-1</sup>  
112 solution DTZc in absolute ethanol for 30 min at room temperature. Modified supports were  
113 then cleaned by successive immersions in water, in sodium hydroxide 10 mM, in water, in  
114 ethanol and in water again, and kept at 4 °C until use.

115

## 116 2.4 Detection

117 Elution of modified supports after mercury extraction was carried out with a 0.5% m/v solution  
118 prepared from L-cysteine.

119 For CV-AAS detection, a 6 mol.L<sup>-1</sup> solution of hydrochloric acid (trace metal grade) was used  
120 with a 0.135 mol.L<sup>-1</sup> solution of sodium borohydride prepared in 0.125 mol.L<sup>-1</sup> sodium  
121 hydroxide solution.

122 Concerning the colorimetric detection, a post-elution photo-oxidation step was first performed  
123 using hydrogen peroxide and hydrochloric acid in order to obtain a final concentration of 0.5  
124 mol.L<sup>-1</sup> of each reagent in the eluent. At the end of the photo-oxidation step, a 1.1 mol.L<sup>-1</sup>  
125 solution of ascorbic acid was then added to eliminate the excess of hydrogen peroxide before  
126 detection. The final colorimetric reagent was prepared according to the conditions described by  
127 Theraulaz et al. [20] with a 0.01 mmol.L<sup>-1</sup> solution of dithizone prepared in a 0.01 mol.L<sup>-1</sup>  
128 glycine buffer solution with 30% ethanol v/v, and mixed with a 0.001 mol.L<sup>-1</sup> thiourea solution  
129 (Sigma-Aldrich, USA).

130

## 131 2.5. Apparatus

### 132 2.5.1. *Metal analysis*

133 Cold vapour atomic absorption spectrometry (CV-AAS) was used to quantify mercury in  
134 standard solutions and real samples. The measurements were carried out on a Thermo Scientific  
135 ICE3500 (USA) atomic absorption spectrometer equipped with a mercury hollow-cathode lamp  
136 operated at 6 mA (wavelength of 253.7 nm) and a VP 100 Vapour System, with a peristaltic  
137 pump operated at 30 rpm. Determinations were carried out with the following parameters: acid  
138 flow rate 0.7 mL.min<sup>-1</sup>, reductant flow rate 1.6 mL.min<sup>-1</sup>, sample flow rate 7.0 mL.min<sup>-1</sup>,  
139 measuring time 6 seconds, argon flow rate 104 mL.min<sup>-1</sup>.

140 Interferences of other metals on mercury extraction/elution were studied by inductively coupled  
141 plasma–atomic emission spectrometry (ICP–AES) with a Jobin YVON JY2000 Ultratrace  
142 spectrometer, equipped with a CMA spray chamber and a Meinhard R50-C1 glass nebuliser.  
143 Determinations were performed with the following settings: power 1000W, pump speed 20  
144 mL.min<sup>-1</sup>, plasma flow rate 12 L.min<sup>-1</sup>, coating gas flow rate 0.15 L.min<sup>-1</sup>, nebuliser flow rate  
145 1.08 L.min<sup>-1</sup> and nebuliser pressure 2.6 bar.

146

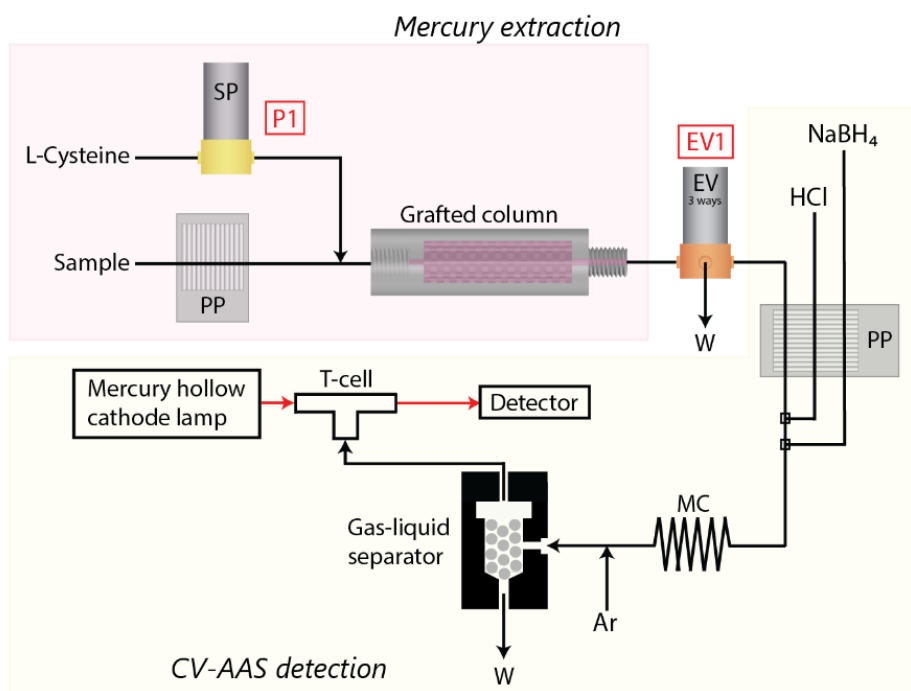
### 147 2.5.2. *3D printing*

148 The DTZc grafting procedure was optimized on 3D printed disks and cuboids. These pieces  
149 were designed with Rhinoceros® 5.0 3D software (Robert McNeel & Associates Europe,  
150 Spain) and then printed on the Form1+ stereolithographic printer (Formlabs, USA), using an  
151 acrylate/methacrylate transparent resin (Clear, BV-002, Formlabs, USA). The integration of  
152 amines functions and the DTZc grafting were first tested and optimized on 3D printed disks  
153 (diameter 19 mm, thickness 2 mm) in batch experiments. Then the optimized parameters were  
154 applied on a cuboids' column (14.1 x 54.1 mm, 284 cubes with a 1.5 mm diameter) which had  
155 a grafted surface of 37.2 cm<sup>2</sup>.

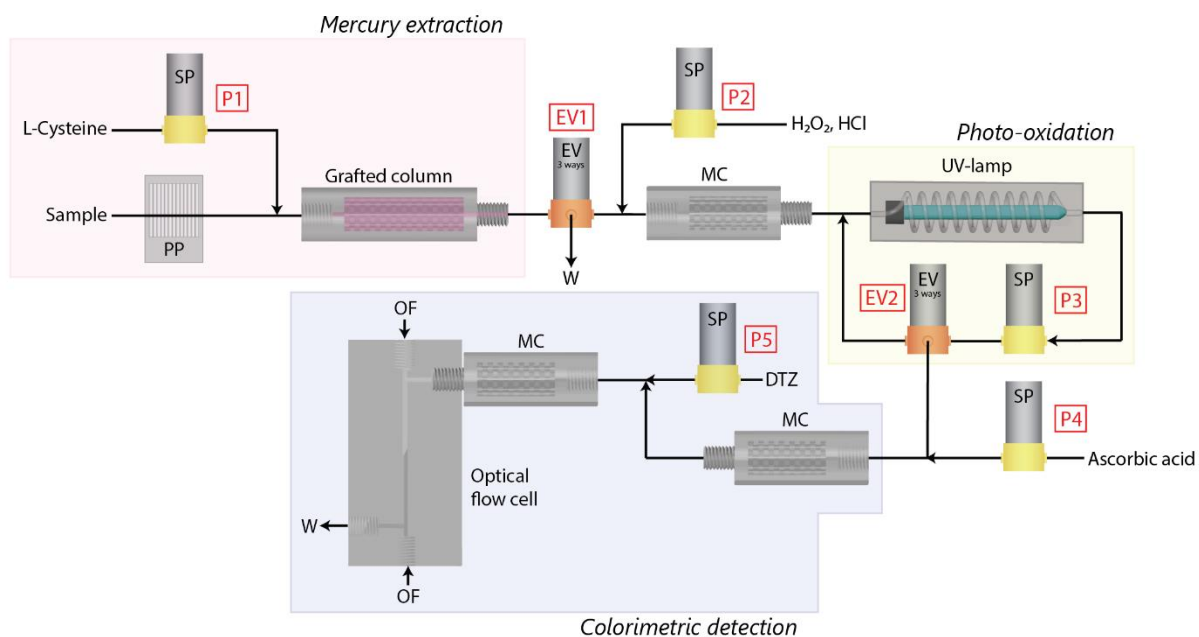
156

### 157 2.5.3. *Flow systems*

158 Sample was propelled using a peristaltic pump (Labcraft, Armtop, France). Reagents were  
159 introduced by means of solenoid micro-pumps (Bio-ChemValve Inc., USA) with a stroke  
160 volume of 20 µL and a highest frequency of 250 cycles/min and 3-way solenoid valves  
161 (Takasago Electric Inc., Japan). The pumps and valves were computer-controlled by a  
162 MCFIA/MPFS system (Sciware, Spain) with eight digital 12V output channels. Two flow  
163 systems were developed according to the detection method used (CV-AAS or colorimetry),  
164 their operating scheme is presented in Fig. 1 and Fig. 2.



165  
 166 **Figure 1:** Flow system for mercury determination with CV-AAS detection [P1: solenoid micropump; PP:  
 167 peristaltic pump; EV: solenoid valve; MC: mixing coil; W: waste; OF: optical fiber; Ar: argon].  
 168



169  
 170 **Figure 2:** Flow system for mercury determination with colorimetric detection [P1-P4: solenoid micropumps; PP:  
 171 peristaltic pump; EV: solenoid valve; MC: mixing coil; W: waste; OF: optical fiber; DTZ: dithizone].  
 172

173 In both systems, the first step of the analytical procedure was the mercury extraction from the  
 174 sample (PP and EV1 to waste) on the DTZc grafted 3D printed cuboid column. Then, a solution  
 175 of L-cysteine was pumped (P1) to elute the mercury extracted onto the grafted column.

176 The first system included a CV-AAS detection system directly after the elution step, previously  
177 described in section 2.5.1 (Fig. 1).

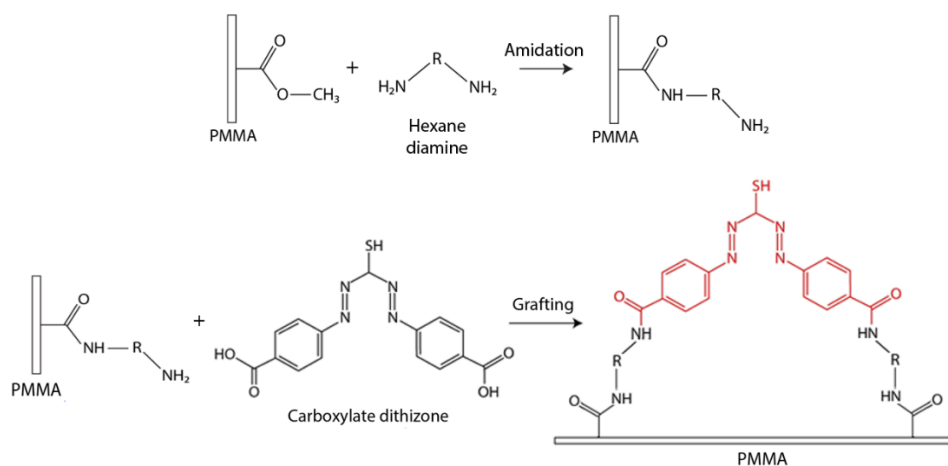
178 The second system offered a simple colorimetric detection (Fig. 2). This detection was based  
179 on a photo-oxidation step to liberate the mercury from L-cysteine before a final colorimetric  
180 detection with a dithizone reagent. A photo-oxidation module was used with a low-pressure  
181 mercury lamp emitting at 254nm (90%) and 185 nm (10%), with a radiating part of 22.86 cm  
182 in height and 0.95 cm in diameter, covered by a Suprasil quartz loop with an inner diameter of  
183 2 mm (UVP PenRay, USA). Hydrogen peroxide oxidant solution (P2) was added to the eluate  
184 to enhance photo-oxidation of L-cysteine and the mixture was exposed under UV-lamp for 30  
185 minutes (P3 and EV2). An ascorbic acid solution (P4) was added at the end of this step to  
186 eliminate excess of oxidant. The dithizone reagent (P5) was introduced in the system for the  
187 detection of dithizone-mercury complex at 480 nm. Detection was carried out in a black 3D  
188 printed spectroscopic flow-cell with a 5 cm optical pathlength. Two FC-UV600 optical fibers  
189 (OF) (Ocean Optics, USA) were connected at the ends of optical pathlength, and isolated from  
190 the reaction mixture with two tailor-made quartz discs, to guide the light from the source to the  
191 spectrophotometric detector. The radiation of the halogen bulb of a DH-2000 UV-Vis light  
192 source (Ocean Optics, USA) was transmitted to a USB2000 miniature spectrometer detector  
193 (Ocean Optics, USA). The whole system was controlled by AutoAnalysis 5.0 software  
194 (Sciware, Spain).

195

### 196 3. Results and discussion

#### 197 3.1. Modification of 3D printed device

198 Stereolithography resins are mainly composed of methyl methacrylate, which is an ester  
199 monomer. After photopolymerization and poly(methyl methacrylate) (PMMA) formation, this  
200 ester group can be used to graft molecules onto the surface of 3D printed objects. This grafting  
201 procedure requires two steps (global procedure is summarized in Fig. 3): first amine functions  
202 were introduced onto 3D printed surface by amination reaction of the ester functions of the  
203 PMMA with hexane diamine [21], followed by grafting of DTZc using an amidation reaction  
204 with carboxylate function of DTZc. A pink coloration of the solid surface after cleaning at the  
205 end of the procedure demonstrates efficiency of the DTZc grafting (supplementary materials  
206 Fig. S1).



207

208 **Figure 3:** Grafting pattern of DTZc onto PMMA.

209 These two steps were optimized in batch experiments on 3D printed disks thanks to the results  
 210 of ADECA test (Amino Density Estimation by Colorimetric Assay). This test allows  
 211 quantification of the amine functions on a solid surface [22]. A chromogenic reagent, the  
 212 Coomassie brilliant blue, reacts with amine functions in acidic medium. Then the quantity of  
 213 Coomassie brilliant blue which has reacted with the amine functions is extracted in basic  
 214 medium and finally quantified by colorimetric detection in acidic medium at a wavelength of  
 215 611 nm.

216

### 217 3.1.1. PMMA amination step

218 The PMMA amination step was carried out according to the method previously described by  
 219 Fixe et al. [21] with a heated solution of hexane diamine in borate buffer (pH=11.5). 3D printed  
 220 disks were immersed in this solution with a reaction time between 30 min and 4 h. Three  
 221 parameters were studied by a one-factor-at-a-time method: temperature, percentage of hexane  
 222 diamine in solution, and time. The results of ADECA test obtained with the various operating  
 223 conditions are summarized in Table 1 (the higher the result of ADECA test, the better the  
 224 efficiency of the amination step). The results showed first the advantage of heating the hexane  
 225 diamine solution to at least 50°C. There was no significant difference between 50 and 70°C  
 226 with  $1.42 \pm 0.04$  and  $1.48 \pm 0.05$  respectively. Moreover, the 3D printed disks have shown signs  
 227 of premature aging at 70°C with undesired cracking on the surface. Consequently, a temperature  
 228 of 50°C was chosen as the optimal condition. Concerning the other parameters, a 10% m/v  
 229 hexane diamine solution and a reaction time of 1 h were the best conditions to obtain a  
 230 maximum amination efficiency ( $1.75 \pm 0.13$ ).

231

232

233 **Table 1.** Optimization of the PMMA amination reaction according to the ADECA test (n=3)

Operating conditions	Quantity of NH <sub>2</sub> functions	
	ADECA test (a.u.)	
Temperature (°C)	25	$1.26 \pm 0.15$
	50	$1.42 \pm 0.04$
	70	$1.48 \pm 0.05$
Hexane diamine concentration (% m/v)	10	$1.75 \pm 0.13$
	15	$1.43 \pm 0.04$
	20	$1.41 \pm 0.06$
	25	$1.24 \pm 0.06$
Amination time (h)	0.5	$1.02 \pm 0.06$
	1	$1.75 \pm 0.13$
	2	$1.27 \pm 0.02$
	4	$1.11 \pm 0.05$

234

235

### 236 3.1.2 DTZc grafting

237 The DTZc grafting was studied after amination of 3D printed disks according to the best  
 238 operating conditions described previously. Four parameters have been optimized by a one-



239 factor-at-a-time method: activating agents (EDC and HOBt) concentration, DTZc  
 240 concentration, temperature and grafting time. The influence of each parameter on the grafting  
 241 efficiency was evaluated based on the results of the ADECA test. In this case, a low value of  
 242 the ADECA test indicates a good efficiency of the grafting reaction, as it shows a decrease in  
 243 the number of free amine groups onto the PMMA surface.

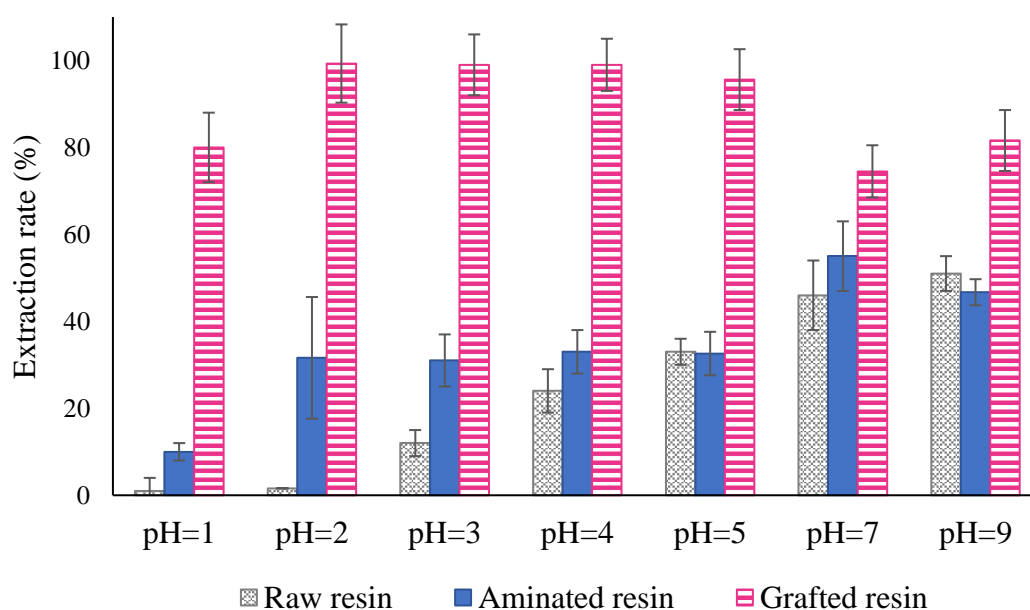
244 The results are summarized in Table 2. Concerning activating agents EDC and HOBt, a  
 245 concentration of 5 g.L<sup>-1</sup> for both reagents was enough to obtain the best grafting rate (0.32 ±  
 246 0.01). For the DTZc concentration, we observed no significant difference between 1 and 2.5  
 247 g.L<sup>-1</sup> (with ADECA test results at 0.35 ± 0.02 and 0.33 ± 0.03 respectively). A concentration of  
 248 1 g.L<sup>-1</sup> was thus selected for further experiments in order to limit the consumption of the reagent.  
 249 No effect of temperature has been observed and the grafting reaction could therefore be  
 250 performed at room temperature (25°C). Finally, a minimum reaction time of 30 min was  
 251 necessary to obtain a good grafting efficiency and no significant difference was observed  
 252 between 30 and 60 min.

253  
 254 **Table 2.** Optimization of the PMMA grafting reaction [EDC: N-(3-Dimethylaminopropyl)-N'-ethylcarbodiimide;  
 255 HOBt = 1-Hydroxybenzotriazole; DTZc = dicarboxylate 1,5-diphenyl-3-thiocarbazone] (n=3)

Operating conditions	Quantity of NH <sub>2</sub> functions ADECA test (a.u.)	
EDC/HOBt concentration (g.L <sup>-1</sup> )	5	0.32 ± 0.01
	10	0.37 ± 0.03
	20	0.37 ± 0.05
	40	0.38 ± 0.03
DTZc concentration (g.L <sup>-1</sup> )	1	0.35 ± 0.02
	2.5	0.33 ± 0.03
	5	0.43 ± 0.02
	10	0.77 ± 0.04
Temperature (°C)	25	0.35 ± 0.02
	40	0.35 ± 0.02
	60	0.37 ± 0.02
Grafting time (min)	10	0.80 ± 0.11
	30	0.31 ± 0.02
	60	0.31 ± 0.02

256  
 257  
 258 **3.2. Solid phase extraction of mercury on grafted 3D printed device**  
 259 *3.2.1 Extraction of metals*  
 260 Shenashen et al. [19] have previously demonstrated that mercury was bonded to two molecules  
 261 of DTZc through S and one N atom, which is consistent with dithizone reactivity, a well-known  
 262 ligand which forms ML<sub>2</sub> complexes with various metals (including mercury) through S and N  
 263 bonding.

264 After the optimization of the grafting procedure, mercury extraction was studied following  
 265 various conditions. Raw resin, aminated resin, and grafted resin disks were immersed for 1 h in  
 266 a  $100 \mu\text{g.L}^{-1}$  mercury solution in PTFE tubes, at pH values between 1 and 9. The mercury  
 267 solution was analysed by CV-AAS before and after extraction. The results obtained (extraction  
 268 rate calculated from the concentrations before and after extraction) are summarized in Fig. 4.  
 269 For pH value above 4, an average extraction of 38% of mercury by raw resin was observed (min  
 270 24% at pH = 4; max 51% at pH = 9), which is characteristic of the adsorption of a metal on a  
 271 plastic material surface, as it was previously demonstrated for polyethylene [23]. In acidic  
 272 medium (pH=2), mercury was thus not extracted by the raw resin material (less than 1%): this  
 273 result shows the importance to work at acidic pH to avoid the contamination of 3D printed  
 274 pieces during the flow procedure. Aminated resin disks also showed a partial extraction of  
 275 mercury in a pH range between 2 and 9, probably due to the complexation of mercury by the  
 276 amine functions (min 32% at pH = 2, max 55% at pH = 7).  
 277

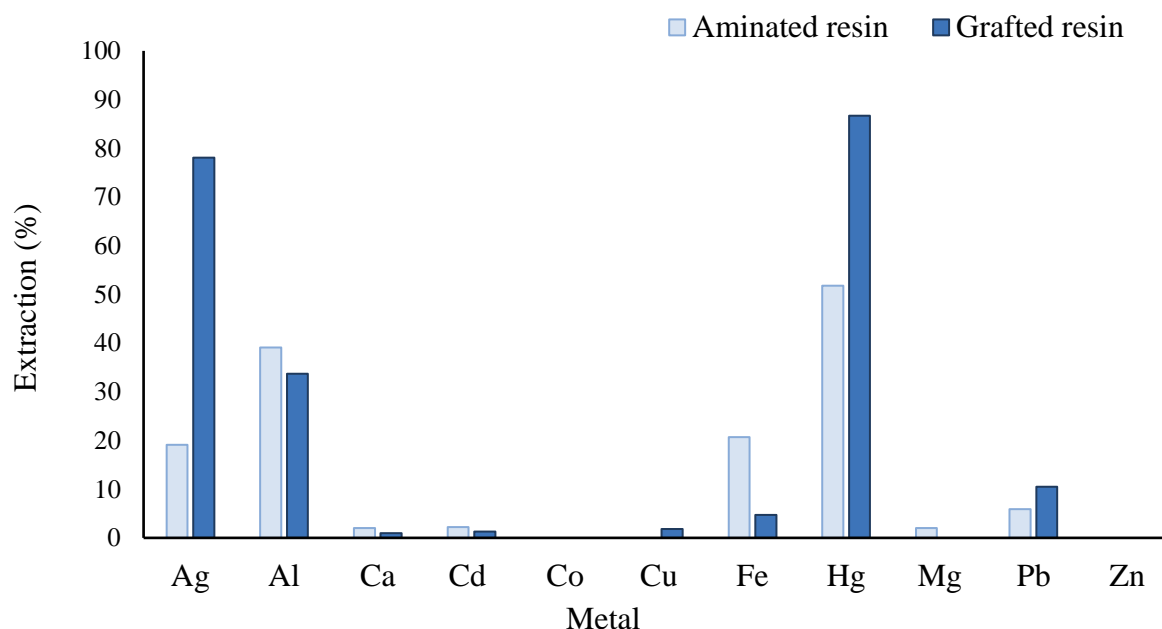


278  
 279 **Figure 4:** Batch extraction of a  $100 \mu\text{g.L}^{-1}$  mercury solution ( $V=50 \text{ mL}$ ) on raw resin, aminated resin and DTZc  
 280 grafted resin disks versus pH ( $n=3$ ).  
 281

282 Results showed complexation of mercury by DTZc onto the surface of disks, as shown by the  
 283 significant increase of extraction rate between the raw resin disks and the grafted resin disks at  
 284 acidic pH values. Concerning the grafted resin disks, the extraction in acidic medium was very  
 285 efficient, with a mercury extraction rate of 99%. The acidification of the samples at pH=2 before  
 286 extraction by the grafted resin was the best compromise to obtain good extraction performance  
 287 and to avoid adsorption phenomena on the plastic surfaces. At this pH value, extraction kinetics  
 288 was rapid since a mercury extraction rate of 90% was reached after a contact time of 1 minute  
 289 (supplementary materials Fig. S2).

290 The selectivity of the DTZc grafted resin was tested with a multi-metal solution (aluminium,  
 291 calcium, cadmium, cobalt, copper, iron, lead, magnesium, mercury, silver and zinc) at pH=2.  
 292 This solution was extracted on the aminated and the grafted resins, and solutions were analysed

293 by ICP-AES before and after extraction (Fig. 5). The results showed a good extraction of silver,  
 294 a partial extraction of aluminium and a low extraction of lead both for aminated and grafted  
 295 resins. Iron was also partially extracted on the aminated resin (20%), but extraction rate on  
 296 DTZc grafted resin was below 5%.  
 297



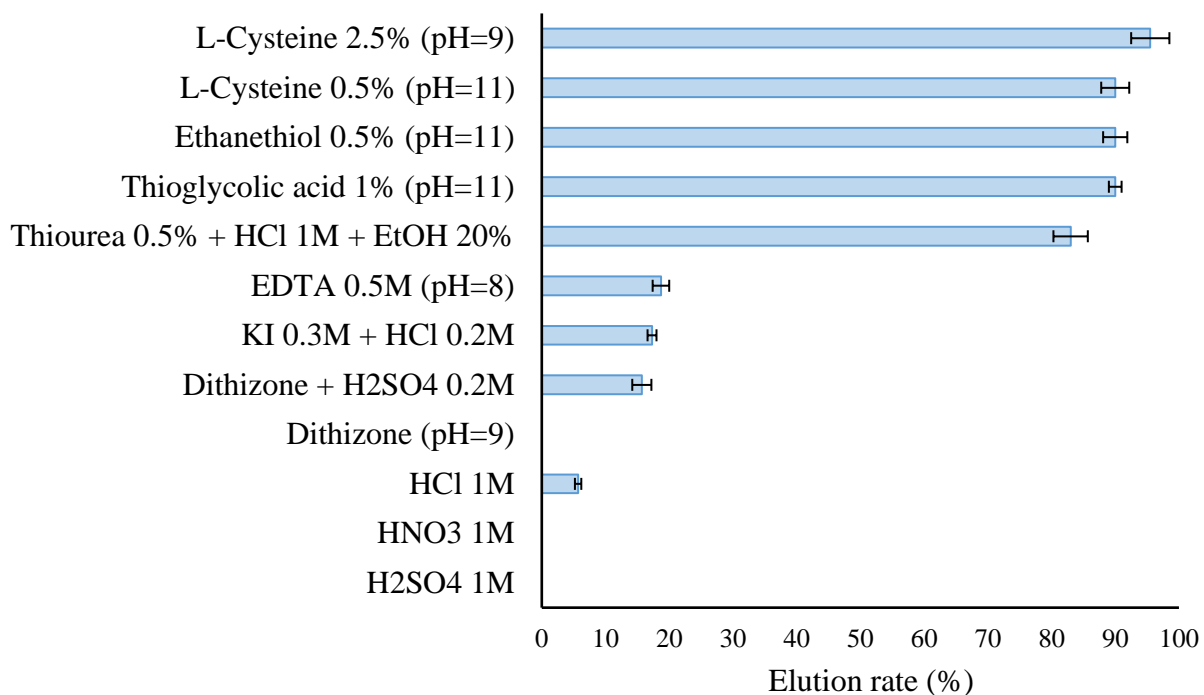
298  
 299 **Figure 5:** Batch extraction of a multi-metal solution at  $10 \mu\text{mol.L}^{-1}$  (aluminium, calcium, cadmium, cobalt, copper,  
 300 iron, lead, magnesium, mercury, silver, and zinc;  $V=50 \text{ mL}$ ) at  $\text{pH}=2$  on the aminated resin disks and the grafted  
 301 resin disks.  
 302

303 Three metals presented thus a noticeable affinity with the DTZc grafted resin: silver, aluminium  
 304 and lead. These interferences will be eliminated during the detection step: in the first flow  
 305 system the colorimetric dithizone reagent contains a masking agent (thiourea) to limit foreign  
 306 ions interferences, especially for silver, and in the second system the CV-AAS is a selective  
 307 analytical method for Hg.  
 308

### 309 3.2.2 Elution

310 After the extraction step, it was necessary to find a suitable eluent to recover the mercury  
 311 extracted by the DTZc grafted resin. Several reagents were studied, and the tests are  
 312 summarized in Fig. 6 (elution rates were calculated by the difference between the amount of  
 313 mercury extracted on the grafted supports and the amount of mercury in the eluate solutions).  
 314 Inorganic acids (hydrochloric, sulfuric and nitric acid), which are well known eluents for  
 315 metals, were not efficient to elute mercury, even with  $1 \text{ mol.L}^{-1}$  concentration (higher  
 316 concentrations were not tested to avoid the 3D resin degradation). Dithizone, EDTA and  
 317 potassium iodide were also tested, but resulted respectively in 16%, 19% and 18% elution rates.  
 318 Several eluents with thiol or thiocarbonyl functions were also studied: L-cysteine, ethanethiol,  
 319 thioglycolic acid and thiourea. These four reagents were very efficient to elute mercury with  
 320 elution rates higher than 90 %, except thiourea with 83%. These results are consistent with the  
 321 high mercury affinity for thiolate compounds (R-SH) [24]. Recently Liem-Nguyen et al. [25]  
 322 determined a formation constant of  $\text{Hg(L)}_2$  complexes with cysteine and thioglycolic acid of

323 41.5 and 37.5 respectively. The three thiol compounds tested showed almost identical elution  
 324 rates, and L-cysteine was chosen for further experiments as the least toxic and malodorous  
 325 sulfur compound.  
 326



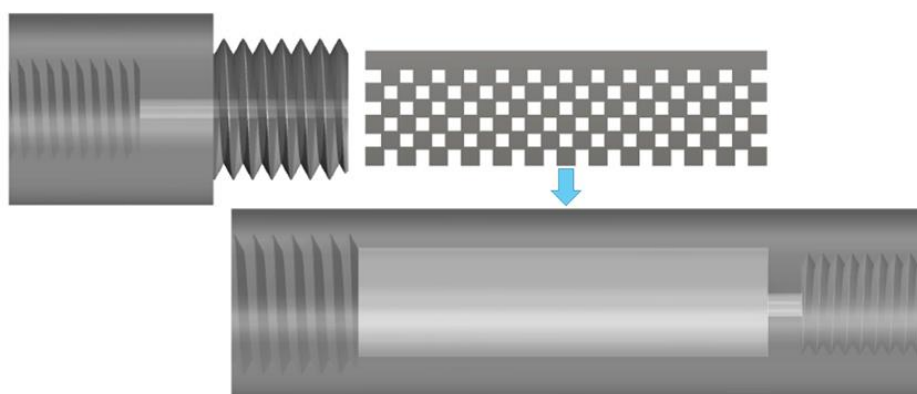
327  
 328 **Figure 6:** Batch elution of mercury extracted on DTZc grafted resin with different eluents (V=50 mL; n=3).  
 329

330 3.3. Application

331 3.3.1. Off-line sampling

332 Given the difficulties of on-site analysis of mercury and real sample storage for further  
 333 laboratory analysis, a cuboid column was used to carry out on-site mercury extraction. For this  
 334 purpose, a column was developed to incorporate a removable rectangular assembly of grafted  
 335 cuboids (Fig. 7), these latter ones being able to be changed for each sample.  
 336

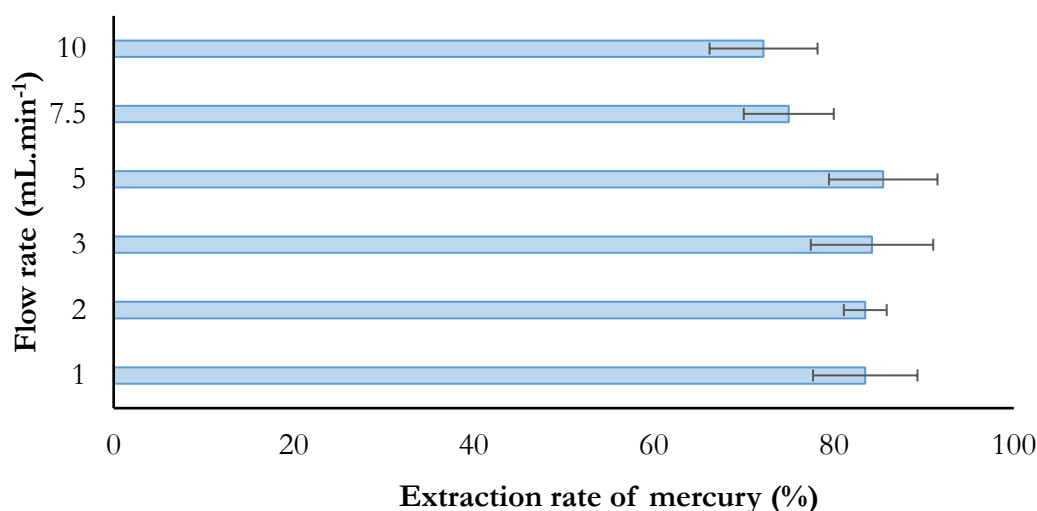
337



338  
 339 **Figure 7:** Scheme of removable column of grafted cuboids.  
 340

341  
 342

343 To optimize the efficiency of the extraction step, the mercury extraction flow rate was studied  
 344 between 1 and 10 mL.min<sup>-1</sup> by means of a peristaltic pump. The results are depicted in Fig. 8.  
 345 Flow rate showed no significant effect on extraction rate between 1 and 5 mL.min<sup>-1</sup> with an  
 346 average mercury extraction rate of 85%. Comparison of extraction efficiency versus higher  
 347 sample flow rates showed a 12% and 17% decrease respectively for sample flow rates of 7.5  
 348 mL.min<sup>-1</sup> (mercury extraction rate of 75%) and 10 mL.min<sup>-1</sup> (mercury extraction rate of 72%).  
 349 Nevertheless, despite the 17% loss, a sample flow rate of 10 mL.min<sup>-1</sup> could be a good  
 350 compromise between the extraction efficiency and the extraction time (or sample volume). A  
 351 sample flow rate of 10 mL.min<sup>-1</sup> enables in a given time a significant increase of the  
 352 preconcentration factor by percolating higher volumes of sample. For a 1 h sample percolation,  
 353 a preconcentration factor of 23 is thus obtained for a sample flow rate of 5 mL.min<sup>-1</sup> versus 38  
 354 for a sample flow rate of 10 mL.min<sup>-1</sup>.  
 355



356 **Figure 8:** Influence of flow rate on the extraction of a 100 µg.L<sup>-1</sup> mercury solution in a grafted cuboids column  
 357 (n=3).  
 358

359  
 360 After the extraction step, the entire cuboids assembly can be removed from the column and  
 361 introduced in a nickel boat of a mercury analyzer Altec AMA 254 which is specifically  
 362 conceived for the fast, precise and simple determination of mercury traces in solids samples.  
 363 Note that with this technique, it was necessary to perform a blank on grafted cuboids before  
 364 extraction, because the analysis of the raw resin used for 3D printing has showed a mercury  
 365 concentration of 9.6 ± 3.2 ng.g<sup>-1</sup>.  
 366

### 367 3.3.2. Flow systems

368 Mercury can also be quantified in solution after elution by L-cysteine by CV-AAS (Fig. 1). As  
 369 the mercury concentration is usually low in environmental samples, it is necessary to work with  
 370 large sample volumes to achieve a large preconcentration factor. In this study, the sample  
 371 volume was set at 500 mL to limit the analysis time (mercury extraction was successfully tested  
 372 for sample volumes up to 1 L). Experiments were carried out to determine the minimum volume  
 373 of L-cysteine which has to be used to quantitatively elute the mercury extracted on modified  
 374 supports. Results showed that a minimum volume of 10 mL of 0.5% m/v L-cysteine in borate

375 buffer (pH=11) should be used to elute 92% of the mercury extracted on the modified support  
376 (Supplementary materials, Figure S3).

377 The analytical features of this procedure were thus determined for a sample volume of 500 mL  
378 and an elution volume of 10 mL: a limit of detection (LOD,  $3\sigma$ ;  $n=10$ ) of  $2.6 \text{ ng.L}^{-1}$  and a limit  
379 of quantification (LOQ,  $10\sigma$ ;  $n=10$ ) of  $8.6 \text{ ng.L}^{-1}$  were achieved, with a linear range from 8.6  
380 to  $200 \text{ ng.L}^{-1}$ . The overall analysis time by this analytical procedure was 60 minutes. The 3D  
381 printed DTZc grafted supports can be reused for 3 successive extractions. The tests showed a  
382 decrease in the extraction rate to 65% from the fourth extraction. This method was validated on  
383 two samples of fresh water and drinking water: as the mercury concentration was below the  
384 LOD, samples were spiked to  $40 \text{ ng.L}^{-1}$ . The results obtained were consistent with  $38.2 \pm 5.1$   
385  $\text{ng.L}^{-1}$  for fresh water and  $44.1 \pm 4.2 \text{ ng.L}^{-1}$  for drinking water (recovery rates ranged from 83%  
386 to 120% in sample replicates).

387 The analytical procedure of the second flow system (Fig. 2) was divided in four steps: extraction  
388 of mercury, elution, photo-oxidation, and colorimetric detection. Dithizone reagent was used  
389 for the mercury detection because of its sensibility to mercury and to avoid interferences with  
390 other extracted metals (silver and aluminium). A linear domain was observed between 1 and  
391  $200 \mu\text{g.L}^{-1}$  for a 500 mL sample volume and a 10 mL elution volume. The limit of detection  
392 was  $0.3 \mu\text{g.L}^{-1}$  ( $n=10$ ), and the limit of quantification was  $1.0 \mu\text{g.L}^{-1}$ . Coefficient of variation  
393 obtained for a mercury concentration of  $50 \mu\text{g.L}^{-1}$  was 2.2%. The overall analysis time by this  
394 analytical procedure was 90 minutes.

395 Given these results, the flow system with colorimetric detection was more intended for analysis  
396 of wastewater or industrial water, while the CV-AAS flow system was most adapted for fresh  
397 water and seawater because of its lower LOD and LOQ.

398

## 399 **Conclusion**

400 In this study, a new possibility offered by 3D printing has been explored. The  
401 acrylate/methacrylate resin can be used as an inert support to graft selective molecules. The two  
402 steps of the grafting procedure were developed and optimized. The first step was the integration  
403 of amine functions on PMMA, followed by reaction between these amine functions and the  
404 carboxylate function of DTZc. A very good extraction of mercury was observed, and the grafted  
405 resin can be eluted with thiol eluents, more particularly with L-cysteine, which has a high  
406 affinity with mercury.

407 A 3D printed column of cuboids has been grafted and several applications of this module have  
408 been presented to show the different opportunities of the grafting of 3D resin. Other molecules  
409 with carboxylate functions could also be grafted by the same procedure for the extraction of  
410 various metals. This type of column (cubes were spaced 1.2 mm from each other) could lead to  
411 many advantages for solid phase extraction: no clogging, use of unfiltered or prefiltered samples  
412 and compatibility with high flow rates.

413

## 414 **Acknowledgment**

415 This work was included in the project "Lab-on-Ship" funded by the French Research Agency  
416 (ANR-14-CE04-0004). The authors are thankful to Françoise Marco-Miralles and Michelle  
417 Brochen from IFREMER for Hg analysis with Altec AMA 254.

418

419 **References**

- 420 [1] E. Pelletier, Mercury-selenium interactions in aquatic organisms: A review, *Marine*  
421 *Environmental Research*. 18 (1986) 111–132. doi:10.1016/0141-1136(86)90003-6.
- 422 [2] Cancer du poumon et exposition professionnelle aux métaux : une revue des études  
423 épidémiologiques - Article de revue - INRS, (2018).  
424 <http://www.inrs.fr/media.html?refINRS=TC%20120> (accessed April 16, 2018).
- 425 [3] C. Freire, R. Ramos, M.-J. Lopez-Espinosa, S. Díez, J. Vioque, F. Ballester, M.-F.  
426 Fernández, Hair mercury levels, fish consumption, and cognitive development in preschool  
427 children from Granada, Spain , *Environmental Research*. 110 (2010) 96–104.  
428 doi:10.1016/j.envres.2009.10.005.
- 429 [4] T. Yorifuji, T. Tsuda, S. Inoue, S. Takao, M. Harada, Long-term exposure to  
430 methylmercury and psychiatric symptoms in residents of Minamata, Japan, *Environment*  
431 *International*. 37 (2011) 907–913. doi:10.1016/j.envint.2011.03.008.
- 432 [5] Prévention du risque chimique - Mercure, cycle et toxicité, (2018).  
433 <http://www.prc.cnrs.fr/spip.php?rubrique42> (accessed April 25, 2018).
- 434 [6] J.C. Varekamp, P.R. Buseck, Global mercury flux from volcanic and geothermal  
435 sources, *Applied Geochemistry*. 1 (1986) 65–73. doi:10.1016/0883-2927(86)90038-7.
- 436 [7] S. Tang, X. Feng, J. Qiu, G. Yin, Z. Yang, Mercury speciation and emissions from coal  
437 combustion in Guiyang, Southwest China., *Environ Res*. 105 (2007) 175–182.  
438 doi:10.1016/j.envres.2007.03.008.
- 439 [8] D.G. Streets, Z. Lu, L. Levin, A.F.H. ter Schure, E.M. Sunderland, Historical releases  
440 of mercury to air, land, and water from coal combustion, *Science of The Total Environment*.  
441 615 (2018) 131–140. doi:10.1016/j.scitotenv.2017.09.207.
- 442 [9] D.G. Streets, H.M. Horowitz, D.J. Jacob, Z. Lu, L. Levin, A.F.H. Ter Schure, E.M.  
443 Sunderland, Total Mercury Released to the Environment by Human Activities, *Environ. Sci.*  
444 *Technol*. 51 (2017) 5969–5977. doi:10.1021/acs.est.7b00451.
- 445 [10] A.N. Anthemidis, G.A. Zachariadis, J.A. Stratis, Development of a sequential injection  
446 system for trace mercury determination by cold vapour atomic absorption spectrometry  
447 utilizing an integrated gas–liquid separator/reactor, *Talanta*. 64 (2004) 1053–1057.  
448 doi:10.1016/j.talanta.2004.05.003.
- 449 [11] H. Erxleben, J. Ruzicka, Atomic Absorption Spectroscopy for Mercury, Automated by  
450 Sequential Injection and Miniaturized in Lab-on-Valve System, *Analytical Chemistry*. 77  
451 (2005) 5124–5128. doi:10.1021/ac058007s.
- 452 [12] L.O. Leal, O. Elsholz, R. Forteza, V. Cerdà, Determination of mercury by multisyringe  
453 flow injection system with cold-vapor atomic absorption spectrometry, *Analytica Chimica*  
454 *Acta*. 573–574 (2006) 399–405. doi:10.1016/j.aca.2006.04.078.
- 455 [13] M. Garrido, M.S. Di Nezio, A.G. Lista, M. Palomeque, B.S. Fernández Band, Cloud-  
456 point extraction/preconcentration on-line flow injection method for mercury determination,  
457 *Analytica Chimica Acta*. 502 (2004) 173–177. doi:10.1016/j.aca.2003.09.070.
- 458 [14] J.F. van Staden, R.E. Taljaard, Determination of Lead(II), Copper(II), Zinc(II),  
459 Cobalt(II), Cadmium(II), Iron(III), Mercury(II) using sequential injection extractions, *Talanta*.  
460 64 (2004) 1203–1212. doi:10.1016/j.talanta.2004.06.020.

461 [15] C. R. Hammerschmidt, K. L. Bowman, M.D. Tabatchnick, C. H. Lamborg, Storage  
462 bottle material and cleaning for determination of total mercury in seawater, *Limnol. Oceanogr.:*  
463 *Methods* 9 (2011) 426-431. doi:10.4319/lom.2011.9.426

464 [16] E. Mattio, F. Robert-Peillard, C. Branger, K. Puzio, A. Margaillan, C. Brach-Papa, J.  
465 Knoery, J.-L. Boudenne, B. Coulomb, 3D-printed flow system for determination of lead in  
466 natural waters, *Talanta*. 168 (2017) 298–302. doi:10.1016/j.talanta.2017.03.059.

467 [17] E. Mattio, F. Robert-Peillard, L. Vassalo, C. Branger, A. Margaillan, C. Brach-Papa, J.  
468 Knoery, J.-L. Boudenne, B. Coulomb, 3D-printed lab-on-valve for fluorescent determination  
469 of cadmium and lead in water, *Talanta*. 183 (2018) 201–208. doi:10.1016/j.talanta.2018.02.051.

470 [18] C. Calderilla, F. Maya, V. Cerdà, L.O. Leal, 3D printed device for the automated  
471 preconcentration and determination of chromium (VI), *Talanta*. 184 (2018) 15–22.  
472 doi:10.1016/j.talanta.2018.02.065.

473 [19] M.A. Shenashen, S.A. El-Safy, E.A. Elshehy, Architecture of optical sensor for  
474 recognition of multiple toxic metal ions from water, *Journal of Hazardous Materials*. 260 (2013)  
475 833–843. doi:10.1016/j.jhazmat.2013.06.025.

476 [20] F. Théraulaz, O.P. Thomas, Complexometric determination of mercury(II) in waters by  
477 spectrophotometry of its dithizone complex, *Microchimica Acta*. 113 (1994) 53–59.  
478 doi:10.1007/BF01243137.

479 [21] F. Fixe, M. Dufva, P. Telleman, C.B.V. Christensen, Functionalization of poly(methyl  
480 methacrylate) (PMMA) as a substrate for DNA microarrays, *Nucleic Acids Res.* 32 (2004) e9.  
481 doi:10.1093/nar/gng157.

482 [22] G. Coussot, C. Perrin, T. Moreau, M. Dobrijevic, A. Le Postollec, O. Vandenabeele-  
483 Trambouze, A rapid and reversible colorimetric assay for the characterization of aminated solid  
484 surfaces, *Anal Bioanal Chem.* 399 (2011) 1061–1069. doi:10.1007/s00216-010-4363-7.

485 [23] A. Turner, L.A. Holmes, Adsorption of trace metals by microplastic pellets in fresh  
486 water, *Environ. Chem.* 12 (2015) 600–610. doi:10.1071/EN14143.

487 [24] P. Pohl, B. Prusisz, Preconcentration of Mercury Using Duolite GT-73 in the Analysis  
488 of Water Samples by Inductively Coupled Plasma Atomic Emission Spectrometry, *Analytical*  
489 *Sciences*. 20 (2004) 1367–1370. doi:10.2116/analsci.20.1367.

490 [25] V. Liem-Nguyen, U. Skyllberg, K. Nam, E. Björn., Thermodynamic stability of  
491 mercury(II) complexes formed with environmentally relevant low-molecular-mass thiols  
492 studied by competing ligand exchange and density functional theory, *Environmental Chemistry*  
493 14 (2017) 243-253doi:10.1071/EN17062.

494



## Modified 3D-printed device for mercury determination in waters

### Supplementary Materials

495  
496  
497 Elodie Mattio<sup>1</sup>, Nadia Ollivier<sup>1</sup>, Fabien Robert-Peillard<sup>1</sup>, Robert Di Rocco<sup>1</sup>, Catherine  
498 Branger<sup>2</sup>, André Margaillan<sup>2</sup>, Christophe Brach-Papa<sup>3</sup>, Joël Knoery<sup>3</sup>, Damien Bonne<sup>4</sup>, Jean-  
499 Luc Boudenne<sup>1</sup>, Bruno Coulomb<sup>1\*</sup>

500  
501 <sup>1</sup> Aix Marseille Univ, CNRS, LCE, Marseille, France.

502 <sup>2</sup> University of Toulon, MAPIEM, La Garde, France.

503 <sup>3</sup> IFREMER, LBCM, Nantes, France.

504 <sup>4</sup> Aix Marseille Univ, CNRS, Centrale Marseille, ISM2, Marseille, France.

505

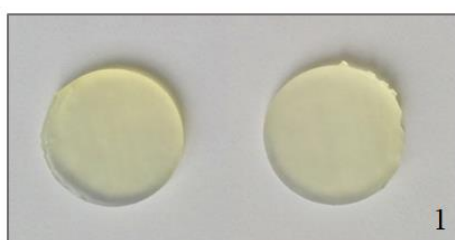
506 \*Corresponding author: bruno.coulomb@univ-amu.fr

507 Full postal address: LCE, Case 29, 3 place Victor Hugo, 13331 Marseille cedex 3, France.

508

509

### Raw resin



511

512

513

514

515



516

517

518

519



520

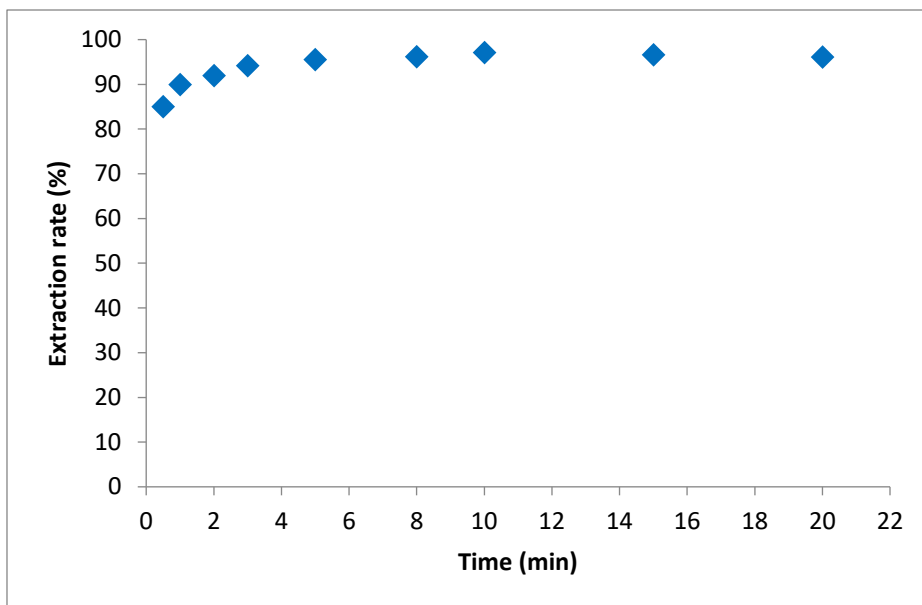
### Grafted resin

521

522 Figure S1: Pictures of 3D printed objects during grafting steps (1: raw resin disks; 2: grafted  
523 resin disks; 3: grafted cuboids columns).

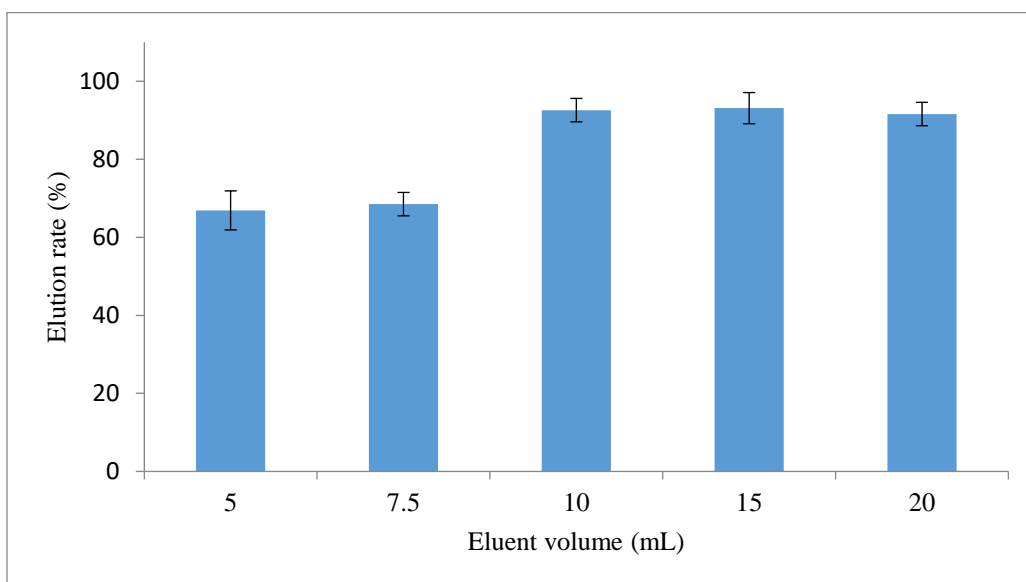
524





525  
526 Figure S2: Extraction rate versus contact time at pH=2.

527  
528



529  
530 Figure S3: Elution rate by L-cysteine versus eluent volume (L-cysteine 0.5% m/v in 100 mM  
531 borate buffer pH=11).

532  
533  
534  
535  
536  
537